JOURNAL OF MATERIALS SCIENCE 27 (1992) 263–269

Influence of shear rate and temperature on the crystallization of spontaneous crystallizing glass-ceramic

T. SEIDEL
Institute of Mechanics, PSF 408, D-9010 Chemnitz, Germany
C. FRIEDRICH
University of Freiburg, Institute of Macromolecular Chemistry, St. Meier Strasse 31, D-7800 Freiburg, Germany

The influence of shear rate and temperature on the viscosity and microstructure of phlogopit glass-ceramic during cooling is investigated. Viscosity was measured in the crystallization temperature range. These experiments were carried out using a high-temperature Couette viscometer specially developed for this investigation. All samples were sectioned, polished, and examined by light microscopy after cooling to room temperature. It is shown that the viscosity of the melt decreases with increasing shear rate because the initial platelets (glimmer crystals) were fragmented by shearing. The resulting glass-ceramic has a high density of broken short crystals. Such a structure has not previously been recorded for this material. A mathematical model to calculate the viscosity of crystallizing glass-ceramic depending on shear rate, temperature and other parameters is presented. This model is based on two modified first-order ordinary differential equations to describe crystal nucleation and crystal growth, and an equation to calculate the viscosity of the resulting suspension. The model also includes a description of crystal fragmentation as a first trial. The equations are coupled by melt viscosity. Numerical solutions are discussed.

1. Introduction

Glass-ceramics have a wide range of practical applications. Usually crystallization occurs after glass-like solidification, but it is also possible to crystallize during cooling in special cases. The latter method is used for investigation of phlogopit glass-ceramic which crystallizes spontaneously and at high velocity. By this method, heat treatment for crystallization after cooling is not necessary. But there are also disadvantages: the usual glass-forming processes are not applicable because viscosity increases sharply with decreasing temperature, and structure and mechanical properties vary uncontrollably due to a variable cooling rate. Therefore it is interesting to investigate both the processing possibilities and methods for improving the structure and properties. In this paper, the influence of shear rate and temperature on both the viscosity of the melt in the crystallization range and the microstructure of the resulting solid is explained.

Only recently have reports appeared in the literature describing studies of materials other than glass-ceramics, especially on metals (for example [1–4]). These papers show how viscosity, microstructure and mechanical properties (strength, ductility, malleability, hardness and impact toughness) can be influenced by shear rate. Due to the formation of a novel structure with nearly spherical particles, sheared material exhibits better and more homogeneous mechanical properties in comparison to conventional materials [4]. New metal-forming processes such as 'rheocasting" were developed. From these results it is reasonable also to investigate glass-ceramic materials, which have the advantage of a lower crystallization velocity than metals; however, the time to influence crystallization by shear rate is longer.

2. Experimental procedure

The glass-ceramic investigated consists of the chemical components listed in Table I [5].

The experiments in the melt were carried out using a high-temperature Couette viscometer specially developed for this purpose. It consists of the following main parts (see Fig. 1):

furnace with siliconcarbide heating elements and a coaxial cylinder system;
motordrive with speed control;
measuring devices for temperature, rotation speed, and torque;
frame.

0022–2461/92 $03.00 + .12

After testing the single parts of the viscometer, the assembly was tested using a glass with known viscosity–temperature characteristics. The experimental data are well in accordance with known characteristics (e.g. see Fig. 3). Into this apparatus the glass-ceramic material was placed in the annular gap between the two cylinders. The inner cylinder was then rotated while the outer cylinder was held fixed. The torque and the speed of the inner cylinder were measured, and shear stress and viscosity, respectively, were calculated using standard relationships considering the geometry of the measuring system. Three different dimensions of rotor and cup were used:

$D_i = 11$ mm, $D_a = 20$ mm; or

$D_i = 12$ mm, $D_a = 20$ mm; or

$D_i = 8$ mm, $D_a = 11$ mm

TABLE I Components of the glass-ceramic studied

Component	Wt %
SiO_2	52.2
Al_2O_3	12.2
Fe_2O_3	8.9
MgO	10.8
Na_2O	9.9
Fluor compounds	5.8
K_2O	0.8
CaO	1.0
MnO	0.1
Total	101.7 (round-up errors)

D_i and D_a are the inside and outside diameters. Shearing length was 40 mm. For further details of the experimental equipment see [6].

Initially, the glass-ceramic powder was completely melted by heating up to a temperature of about 1370 °C, well above its liquidus temperature, T_L, of nearly 1170 °C with a heating rate of 30 K min^{-1}. The sample was held isothermally for about 25 min at that temperature. Three kinds of experiments were then carried out (Fig. 2) [6].

2.1. Experiment A

The sample was continuously sheared between the solidus and liquidus temperatures while cooling at a constant rate (2.44 K min^{-1}). At a temperature above the solidus temperature, the shearing was stopped and the sample was water quenched.

2.2. Experiment B

The sample was cooled with a constant cooling rate (2.44 K min^{-1}) down to a temperature within the liquid–solid range. After reaching the desired temperature, the sample was held isothermally. The rotation speed was then increased and decreased stepwise. Stationary values of torque were measured. After these isothermal experiments, the rotation was stopped and the sample was water quenched.

2.3. Experiment C

The sample was cooled at a constant cooling rate

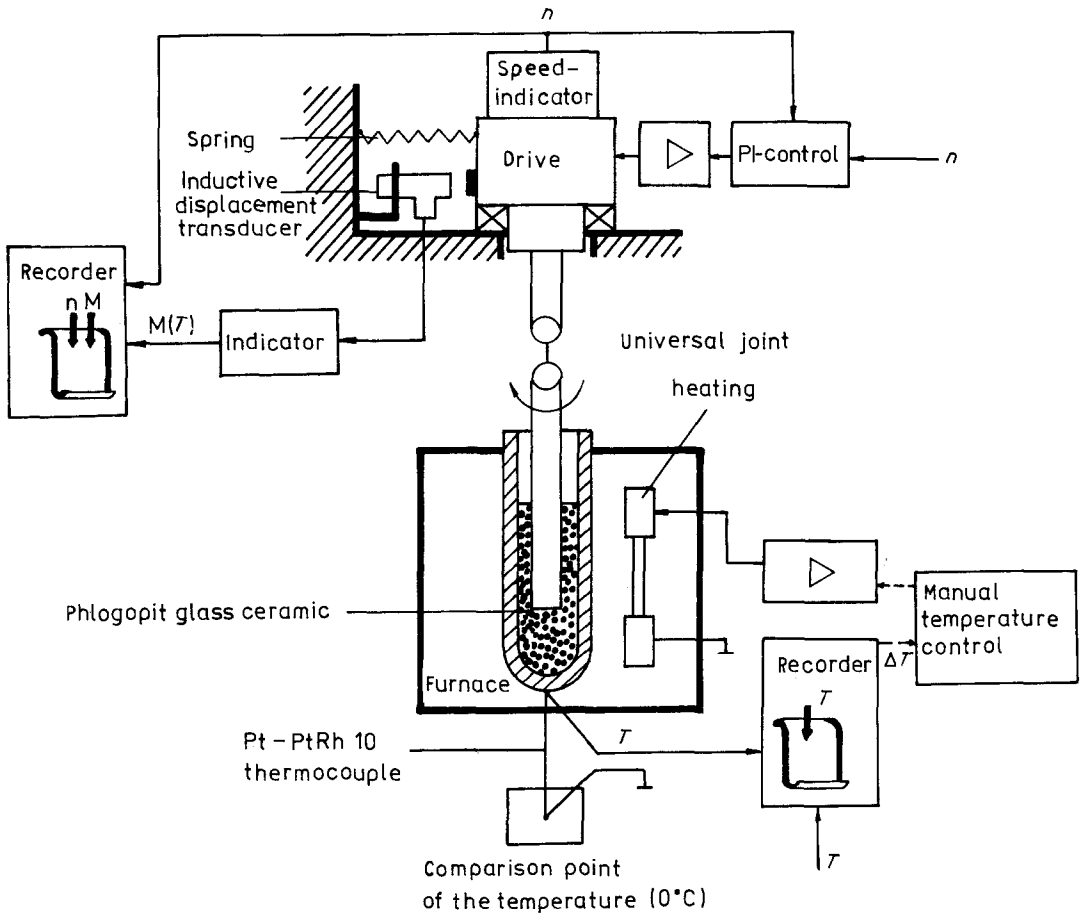

Figure 1 Schematic representation of the experimental apparatus.

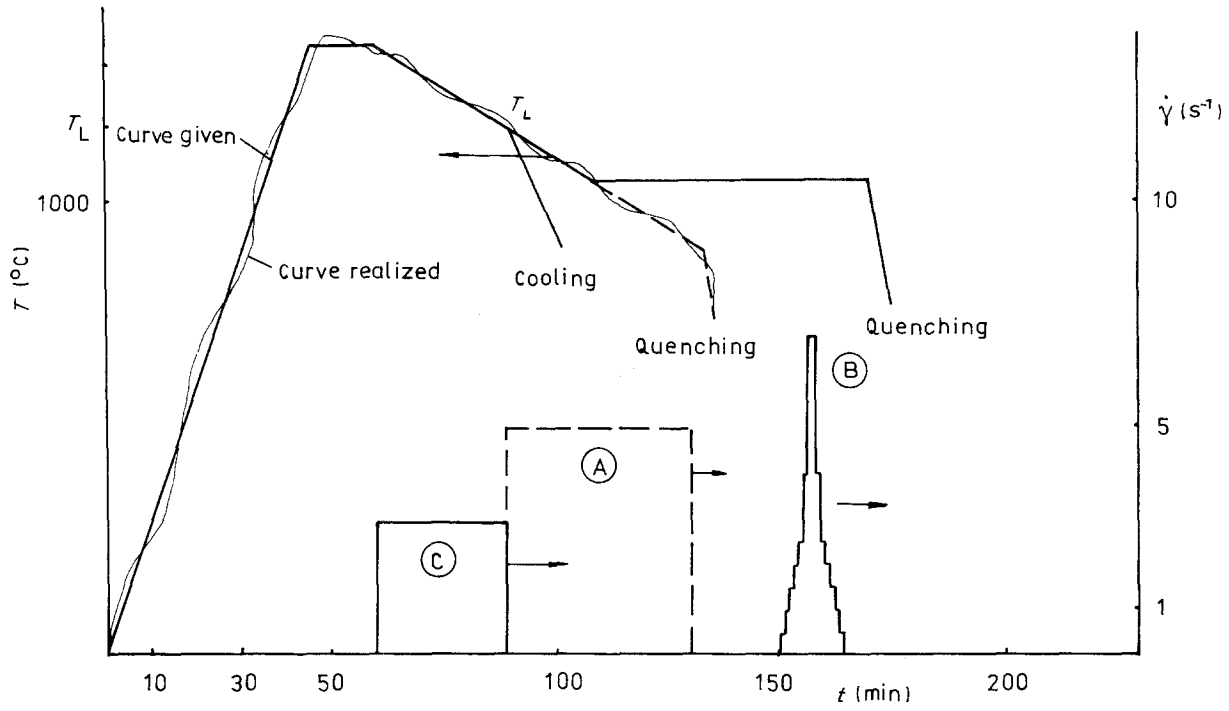

Figure 2 Schematic representation of the thermomechanical treatment for the three kinds of experiment.

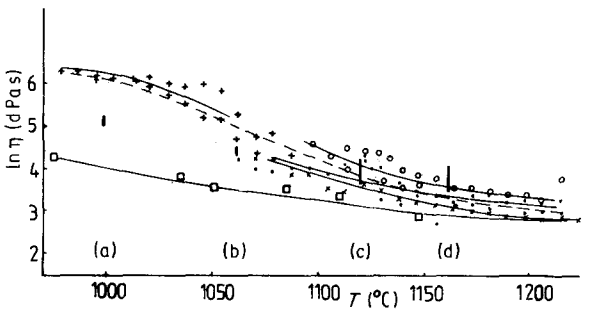

Figure 3 Testing the viscometer with standard glass and showing the dependence of the viscosity of the considered glass-ceramic on temperature for a constant cooling rate of 2.44 K min^{-1} (full and dashed lines) compared to the viscosity measured in the isothermal case (vertical bars). Vertical bars: $\dot{\gamma}$ = (a) 1.0–9.7; (b) 1.7–9.3; (c) 0.4–10.7; (d) 1.5–12.3 s^{-1}. Curves, $\dot{\gamma}$ = ×, 50; ●, 20; ○, 6; +, 0.14 s^{-1}. □, Testing viscometer with standard glass.

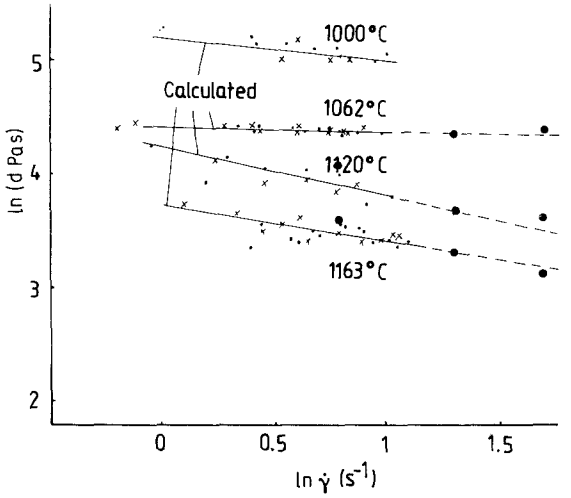

Figure 4 Dependence of the viscosity on shear rate in the isothermal case (crosses and small points) compared to the viscosity for constant cooling rate (large points).

(2.44 K min^{-1}) and sheared above the liquidus temperature. After reaching the liquidus temperature, the heater in the furnace was switched off and the sample was slowly cooled to room temperature.

In all cases the samples were sectioned, polished and examined by light microscopy.

3. Results

Results of typical viscosity measurements are shown in Figs 3 and 4. The individual $\eta - T$ points, seen in the curves in Fig. 3 for constant cooling rate, were fitted by the followng equation

$$\ln \eta = \frac{a}{[T/b]^c + 1} + d \qquad (1)$$

where η is the viscosity and T the temperature. The fit-parameters, a, b, c and d, are given in Table II.

Equation 1 was selected because it is possible to approximate such points using a curve with an inflection point. The influence of the fit parameters on the curve is shown in Fig. 5. The resulting curves for constant shear rates are drawn as thin solid lines. The dashed line represents the shear rate independent fit.

TABLE II Values for the fit parameters of Equation 1

$\dot{\gamma}$ (s^{-1})	a	b	c	d	Availability at temperature T (°C)
0.14	3.929	1075.27	35.122	2.626	979–1084
6.00	3.728	1075.27	29.012	3.259	1097–1216
20.00	2.598	1075.27	20.716	2.904	1063–1282
50.00	3.539	1075.27	18.351	2.437	1071–1282
All data	3.827	1075.27	23.433	2.795	979–1282

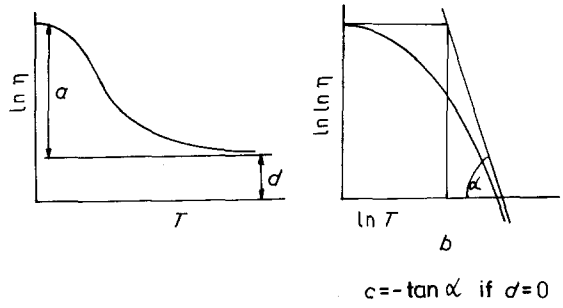

Figure 5 Influence of the parameters for the fit in relation to the points for constant cooling rate.

Notice that viscosity is low at high temperatures and increases with decreasing temperature. This is because both the volume fraction solid, and the viscosity of the remaining glass phase, increase. It is remarkable that the viscosity is lower for high shear rates. It is therefore possible to influence the viscosity by varying the shear rate during cooling. The curves in Fig. 4 show the results of isothermal experiments at four temperatures.

The viscosity of these isothermally held samples, plotted against shear rate on a log–log scale, shows a linear dependence over certain ranges of shear rates. Changes in viscosity with shear rate in Fig. 4 are reversible. The viscosity obeys the classical power-law equation with a negative coefficient n

$$\eta = K\dot{\gamma}^n \qquad (2)$$

The fit parameters, K and n, are shown in Table III.

TABLE III Values for the fit parameters of Equation 2

Temperature (°C)	K (dPa s^{n+1})	n	Availability ($\dot{\gamma}[s^{-1}]$)
962	1.1503×10^6	− 0.2688	0.33– 3.42
998–1002	1.8412×10^5	− 0.248	1.02– 9.69
1062	2.5545×10^4	− 0.0252	1.89– 9.32
1120	1.6788×10^4	− 0.4129	0.37–10.66
1163	5.3040×10^3	− 0.3154	1.54–12.32

For this reason the glass-ceramic shows pseudoplastic behaviour in the crystallization range. In the isothermal case it is also possible to influence the viscosity by varying the shear rate.

Now let us compare the experimental data for the isothermal case with those for constant cooling rate. For this purpose, Figs 3 and 4 include all the pertinent data. Vertical bars in Fig. 3 show the results of isothermal experiments. There seem to be differences between the viscosity of these two types of experiment, especially at low temperatures. The differences are due to different shear rates. The corresponding shear rates of the upper and lower points of the bars are shown in Fig. 3. In Fig. 4, the big points represent the values measured for constant cooling rate: these show nearly the same viscosities as those measured isothermally. Therefore, viscosity depends only on the present shear rate and temperature, and not on thermal and deformation history, for the considered conditions.

The structure of the investigated glass-ceramic at room temperature consists of glimmer crystals and

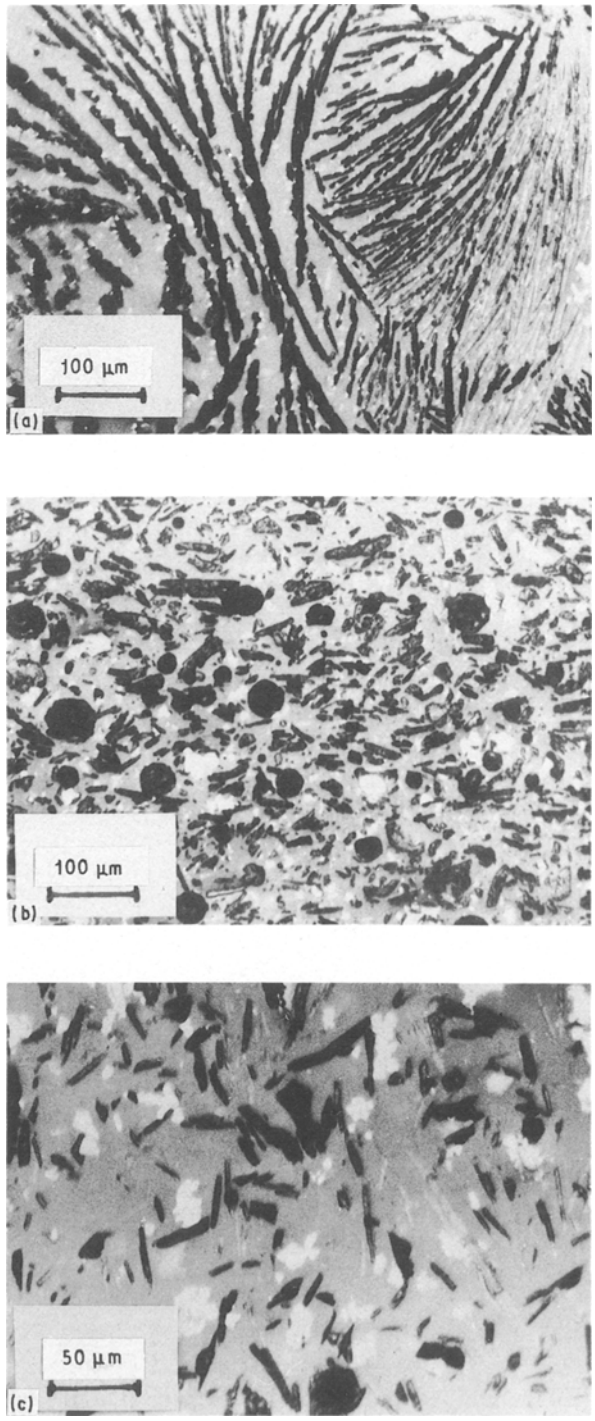

Figure 6 Examples of the structure of both the unsheared and sheared material: (a) Experiment A with $\dot{\gamma} = 0\ s^{-1}$; (b) Experiment A with $\dot{\gamma} = 50\ s^{-1}$, sheared about 70 min during cooling at a constant cooling rate of $\dot{T} = 2.44\ K\ min^{-1}$; (c) Experiment B with $\dot{\gamma}_{max} = 20\ s^{-1}$, sheared about 10 min at 1121 °C.

a surrounding quenched glass matrix. This structure, as well as the rheological behaviour, is markedly changed by shearing. The initial platelet structure is entirely replaced by a structure with broken short crystals. Fig. 6 shows both the conventional platelet-like structure (a) of the glass-ceramic without shearing, and the other new type of structure of the same material sheared in the crystallization temperature range (b, c). This structure has not previously been recorded for the material investigated. Fig. 6b also shows bubbles, which may appear if the material is sheared at more than a critical shear rate and shear time, but

such parameters are not necessary to change the structure.

For shearing above the liquidus temperature (Experiment C) the structure was also changed. A reason for this may be the influence of shear rate on the decomposition of the melt. Changes in structure were lower than in the case of shearing below that temperature, but no direct comparison is possible due to differences in the cooling rate after shearing (quenched or cooled in the furnace). Viscosity measurements above the liquid temperature were impossible because of limitations of the viscometer used.

4. Mathematical model

A dynamic model to calculate viscosity of the crystallizing material is presented. This model is based on equations to describe crystal nucleation and growth, and an equation to calculate the viscosity of suspensions depending on the volume fraction solid. It includes the influence of shear rate on crystallization.

In recent years, numerous studies of crystal nucleation and growth have been made. Most consider a one-component supercooled liquid, and there are often great differences between classical theory and experimental values especially for crystal nucleation. Experimental values are about a factor of 10^{15} to 10^{35} higher for crystal nucleation and about 10^2 higher for crystal growth, in relation to classical theory [7]. To obtain practical, relevant results for the investigated multicomponent glass-ceramic, only the form of the classical theory equations has been taken and modified by an appropriate function depending on processing conditions e.g. $\dot{\gamma}$ (shear rate) and T (temperature). The steady-state rate of heterogeneous crystal nucleation, $\dot{b}_1$, in a one-component supercooled liquid is related to the absolute temperature, T, by the following expression [7–9]

$$\dot{b}_1 = N_V^S \frac{kT}{3\pi L_U^3 \eta_G} \times \exp\left[- c \frac{V_m^2}{(\Delta H_m)^2} \frac{T_L^2}{(T_L - T)^2} \frac{f_{het}}{kT} \right] \quad (3)$$

where $c = (16\pi 6^3/3)$; N_V^S is the number of atoms in contact with the substrate; k is Boltzmann's constant; L_U is the characteristic size of the substrate; V_m is the molar volume; T_L is the liquidus temperature; ΔH_m is the heat of fusion per mole; and η_G is the glass viscosity. The dimensionless function f_{het} ($0 \leqslant f_{het} \leqslant 1$) includes the influence of the substrate. This equation has been modified as follows

$N_V^S = b_1' - b_1$ is variable and will be b_1' under stationary conditions;

b_1' depends on shear rate: increasing the shear rate increases b_1', e.g. $b_1' = b_{10}'[1 + (\lambda_R \dot{\gamma})^{m_{10}}]$. λ_R is a rheological time constant, b_{10}' is a constant.

Glass viscosity, η_G, is replaced by the melt viscosity, η, of the suspension.

Using dimensionless quantities $y_1 = b_1/b_{10}'$, $\theta = T/T_L$, and $h = \eta/\eta_L$ we have

$$\dot{y}_1 = \frac{1}{\lambda_N} \frac{\theta}{h} \exp\left(- \frac{a_{10}}{(1 - \theta)^2 \theta} \right) (g_{10} - y_1) \quad (4)$$

with

$$\lambda_N = \frac{3\pi L_U^3 \eta_L}{kT_L} \quad (4.1)$$

and

$$a_{10} = \frac{16\pi 6^3 V_m^2 f_{het}}{3(\Delta H_m)^2 kT_L} \quad (4.2)$$

where η_L is the viscosity at the liquid temperature T_L; λ_N is a time constant for nucleation; θ is the dimensionless temperature; h is the dimensionless viscosity and a_{10} is a constant. The term $g_{10} - y_1$ represents the influence of shear rate with the following expression for g_{10}

$$g_{10} = 1 + (\lambda_R \dot{\gamma})^{m_{10}} \quad (5)$$

Now let us consider crystal growth. The starting point is an equation developed by Turnbull [10]

$$\dot{b}_2 = b_0 \frac{kT}{3\pi L_{SP}^2 \eta_G} \left[1 - \exp\left(- \frac{\Delta G}{kT} \right) \right] \quad (6)$$

where b_0 is a characteristic crystal size, L_{SP} is a jump distance to the solid–liquid interface, ΔG is the free enthalpy and η_G the glass viscosity. The following modifications were assumed.

1. A size-dependent rate of crystal growth is used in the following form

$$b_0 = b_{00} \left[b_{20} + \left(\frac{b_2}{b_{00}} \right)^{m_{20}} \right] \quad (7)$$

where b_{00}, b_{20} and m_{20} are constants.

2. The glass viscosity, η_G, is replaced by the melt viscosity, η, of the suspension.

3. Dimensionless quantities θ and h, analogous to crystal nucleation and $y_2 = b_2/b_{00}$ (a dimensionless expression for average particle size) were used. Particle-size distribution functions have not been taken into account.

4. The exponential term is replaced by

$$\exp\left(- \frac{(1 - \theta)\, a_{20}}{\theta} \right)$$

where a_{20} is a constant.

5. The influence of shear rate on average size is inserted by two simple functions f_B and f_H.

These modifications lead to the following dimensionless equation

$$\dot{y}_2 = \frac{1}{\lambda_K} \frac{\theta}{h} \left[1 - \exp\left(- \frac{(1 - \theta) a_{20}}{\theta} \right) \right] \times [b_{20} + y_2^{m_{20}}] f_B f_H \quad (8)$$

with

$$\lambda_K = \frac{3\pi L_{SP}^2 \eta_L}{kT_L} \quad (8.1)$$

where λ_K is a time constant. The function f_B is a first trial to describe fragmentation

$$f_B = 1 - \frac{\eta \dot{\gamma}}{\tau_{kr}} \quad (9)$$

which allows negative rates of crystal growth and corresponds to fragmentation, and the function

$$f_H = (1 + \lambda_R \dot{\gamma})^{-1} \quad (10)$$

corresponds to the disturbance of crystal growth by shearing. τ_{kr} is the critical shear stress to break a crystal.

The third problem, in addition to crystal nucleation and crystal growth, is how to calculate the viscosity of these suspensions. The influence of particles suspended in a fluid has received considerable attention in the literature, from both a theoretical and an experimental point of view. There are many equations to calculate the viscosity of suspensions independent of the shape of particles [11–13]. A proven equation is the following, of Maron–Pierce

$$\frac{\eta}{\eta_G} = \left(1 - A\frac{\Phi}{\Phi_{max}}\right)^{-2} \quad (12)$$

where A is a constant, Φ is the volume fraction solid, and Φ_{max} is the maximum loading level, or the geometrical limit for particles in contact with each other in the most efficient packing condition. This is used as the normalizing factor for the volume fraction solid. With the dimensionless expression

$$\frac{\eta_G}{\eta_L} = \exp\left[\frac{(1-\theta)a_{30}}{\theta}\right] \quad (12.1)$$

for the temperature dependence of viscosity, Equation 13 follows

$$h = \exp\left[\frac{(1-\theta)a_{30}}{\theta}\right]\left(1 - \frac{A}{\Phi_{max}} y_1 y_2^{m_{30}}\right)^{-2} \quad (13)$$

where a_{30} and m_{30} are constants.

Equations 4 and 8 are a system of two first-order ordinary differential equations coupled through the melt viscosity with Equation 13. The model includes many parameters, but are not too many in relation to the complexity of the process. For solution, the fourth-order Runge–Kutta method with adaptive step-size control is used [14].

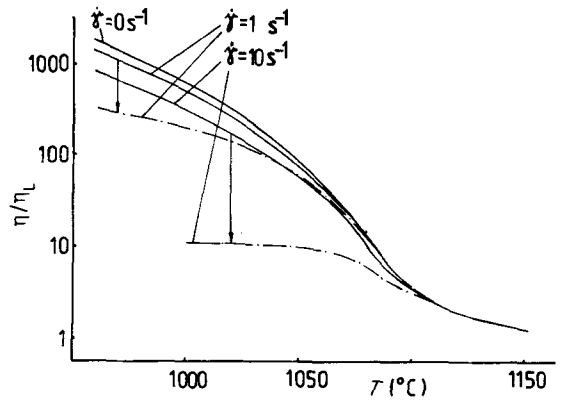

Figure 7 Influence of both shear rate and critical shear stress needed to break crystals, on viscosity–temperature characteristics during crystallization by numerical simulation. $\lambda_N = 3$ s; $\lambda_k = 90$ s; $\lambda_R = 1$ s; $T_L = 1443$ K; $\eta_L = 200$ Pa s; $b'_{10} = 9 \times 10^{17}$ m^{-3}; $a_{10} = 0.01$; $a_{20} = 1$; $a_{30} = 20$; $b_{20} = 1$; $m_{10} = 1$; $m_{20} = 0.3$; $m_{30} = 1$; $\dot{T} = +3$ K min^{-1}. τ_{kr} = ——, 10^{24}; —·—, 10^4 Pa.

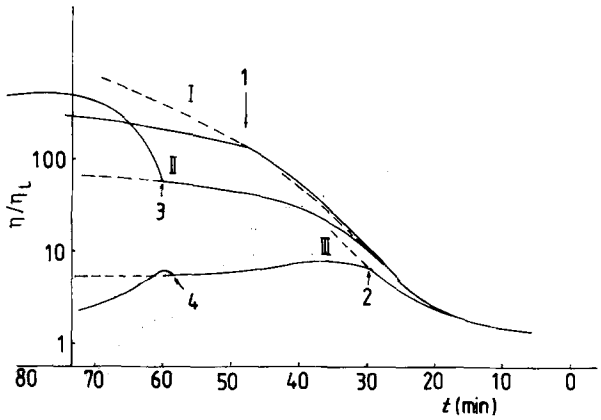

Figure 8 Numerical simulation of time-dependent viscosity in relation to various thermomechanical treatments during crystallization. I, Parameters as in Fig. 7 for $\tau_{kr} = 10^{24}$ Pa; $\dot{\gamma} = 1$ s^{-1}. $\dot{T} = 0$ after time point 1 ($t = 48$ min). II, Parameters as in Fig. 7 for $\tau_{kr} = 10^4$ Pa; $\dot{\gamma} = 1$ s^{-1}. $\dot{T} = 0$ after time point 2 ($t = 30$ min). The shear rate changes up to $\dot{\gamma} = 10$ s^{-1} after time point 3 ($t = 60$ min). III, Parameters as in Fig. 7 for $\tau_{kr} = 10^3$ Pa and $\dot{\gamma} = 1$ s^{-1}. $\dot{T} = 0$ after time point 2 ($t = 30$ min). The shear rate changes up to $\dot{\gamma} = 5$ s^{-1} after time point 4 ($t = 58$ min). Dashed lines represent continuation of curves without described arrangements.

5. Discussion

Figs 7 and 8 show the results of the numerical solution for different cases. The initial conditions are $b_1 = 0$ and $b_2 = 0$ for $t = 0$. The temperature is calculated using cooling rate and time as follows

$$T = T_L - \dot{T}t; \quad \dot{T} = \text{constant} \quad (14)$$

Therefore in the case of $\dot{T} \neq 0$ the temperature and time are equivalent. When $\dot{T} = 0$ this results in a viscosity–temperature dependence. Fig. 7 shows solutions using representative parameters, which are the results of numerical experiments, but are not fitted to the model by mathematical methods. This is a question for further investigations. In this paper only the qualitative effects of the model are discussed. It is seen from Fig. 7 that the viscosity depends on temperature, shear rate, and a critical shear stress for particle fraction. Both increasing shear rate and decreasing critical shear stress lead to decreasing viscosity. There is a qualitative equivalence to the experimental data points in Fig. 3.

Fig. 8 shows the viscosity dependence for various thermomechanical treatments. The first numerical experiment (I) begins with a constant cooling rate ($\dot{T} = 3$ K min^{-1}) and constant shear rate ($\dot{\gamma} = 1$ s^{-1}). After $t = 48$ min, the temperature was held constant. Notice that viscosity increases further because of the increasing volume fraction solid. This is also seen in the second case (II) with other parameters τ_{kr} and $\dot{\gamma}$ after $t = 30$ min. These are changes to a stationary state when $T =$ constant. This period depends differently on the initial conditions. In the second case (II) the shear rate decreases from 1 to 10 s^{-1} after time point 3 ($t_3 = 60$ min). An unrealistic viscosity increase follows. A reason for this is the forced nucleation rate by the parameters used. This increasing viscosity can be compensated by increasing the fraction of crystals

as in case (III): τ_{kr} was reduced to 10^3 Pa. The main conclusion of Figs 7 and 8 is that the model allows any viscosity point below the curve for $\dot{\gamma} = 0$ by varying the thermomechanical treatment.

6. Conclusions

Experiments show that it is possible to influence crystallization of phlogopit glass-ceramic by shearing. The viscosity decreases with increasing shear rate in the crystallization temperature range. This follows also from the mathematical model. By this reasoning, the viscosity is manageable and new processing possibilities may be available, similar to those for metals. Such possibilities are to be investigated in the future. Based on the increase in structural strength of the sheared material in comparison to the unsheared material, one can expect changes in mechanical properties: what changes, and how, remains open for investigation. Last but not least, the mathematical model must be developed with special attention to particle-size distribution and changes in particle form, and the parameters must be fitted to the experimental data.

References

1. T. U. KAUP, PhD Dissertation, TH Aachen, 1989.
2. M. C. FLEMINGS, R. G. RIEK and K. P. YOUNG, *Mater. Sci. Engng* **25** (1976) 103.
3. K. ICHIKAWA and S. ISHIZUKA, *Trans. Jpn Inst. Metals* **28** (1987) 145.
4. N. A. EL-MAHALLAWY, N. FAT-HALLA and M. A. TAHA, in Proceedings of the 4th International Conference on Mechanical Behaviour of Materials, Stockholm, Sweden, 1983, edited by J. Carlsson and N. G. Olson (1983) p. 695.
5. D. REIF, *Sprechsaal* **120** (1987) 510.
6. CH. FRIEDRICH and Th. SEIDEL, Report No. 25/1990 (AdW der DDR, Institut für Mechanik Chemnitz, 1990).
7. U. SCHIFFNER, PhD Dissertation, TU Erlangen, 1984.
8. E. D. ZANOTTO and P. F. JAMES, *J. Non-Cryst. Solids* **74** (1985) 373.
9. E. D. ZANOTTO, *ibid.* **89** (1987) 361.
10. W. VOGEL, Glaschemie (Deutscher Verlag für Grundstoffindustrie, Leipzig, 1979).
11. R. I. TANNER, "Engineering Rheology" (Clarendon Press, Oxford, 1985).
12. A. B. METZNER, *J. Rheol.* **29** (1985) 739.
13. R. K. GUPTA and S. G. SESHADRI, *ibid.* **30** (1986) 505.
14. W. H. PRESS, B. P. FLANNERY, S. A. TEUKOLSKY and W. T. VETTERLING, "Numerical Recipes" (Cambridge University Press, Cambridge, 1986).

Received 6 September 1990
and accepted 28 February 1991